Transmembrane fragment structures of Amyloid Precursor Protein depend on membrane surface curvature

Laura Dominguez,[†] Stephen C. Meredith,[‡] John E. Straub,[*,†] and D. Thirumalai[¶]

Department of Chemistry, Boston University, Boston, MA 02215, Department of Biochemistry and Molecular Biology and Department of Pathology, The University of Chicago, Chicago, IL 60637, and Department of Chemistry and Biochemistry and Biophysics Program, University of Maryland, College Park, MD 20742

Received January 2, 2014; E-mail: straub@bu.edu

Supporting Information Available: *Computational Methods:* Initial conditions for the simulations were taken from experimentally derived structures determined by NMR of $C99_{15-55}$ in zwitterionic dodecylphosphocholine (DPC) micelles (PDB 2LLM).[1] The POPC and DPC all-atom systems were generated using the CHARMM-GUI Membrane Builder[2,3] and modeled using the CHARMM36 all-atom lipid and protein force field and TIP3P water model.[4–6] Parameters for dodecyl phosphocholine lipids for CHARMM36 were taken from Abel.[7] The bilayer system consists of $C99_{15-55}$ monomer, 128 POPC lipids, 5,474 TIP3P water molecules, and 3 Cl^- ions to neutralize the system. The micelle system contained $C99_{15-55}$ monomer, 53 DPC molecules, 17,374 waters, and 3 Cl^- ions to neutralize the system. For comparison, additional simulations were performed using CHARMM36 without the CMAP correction.[6]

A*ll-atom model simulations:* For simulations in the POPC bilayer a total of 100 ns of MD were performed on each system (following minimization and a short NVT and NPT equilibration with protein backbone fixed). The pressure was set to 1 bar using a semi-isotropic coupling scheme with lateral and perpendicular pressures treated separately with coupling time 0.1 ps using the Parrinello-Rahman barostat methodology. The temperature of the system was set to 303 K and regulated using the Nosé-Hoover weak coupling algorithm.[8]

The non-bonded interactions were truncated using shift functions (between 0.9 and 1.2 nm for Lennard-Jones interactions and between 0 and 1.2 nm for electrostatics). Long-range electrostatic interactions were calculated using the Particle Mesh Ewald (PME) method[9] with a Fourier grid spacing of 0.12 nm. The linear constraint solver (Lincs) method[10] was used to constrain all bond lengths, with a 2 fs integration step. All-atom simulations in a DPC micelle were carried out under the same conditions using an isotropic coupling scheme to control the pressure.

The HELANAL program was used to calculate the kink angle along the TM helix between residues K28 and V50.[11] A sliding window of four residues was employed to establish local helical axes, followed by an assessment of the local helical distortion along the length of the helix over time.

The membrane bilayer thickness was measured as the average distance between the z-coordinate of the upper and lower leaflet phosphate, while the micelle thickness was measured as the average radius of gyration of the DPC micelle, by taking the root mean square distance of all DPC atoms from the micelle center-of-mass. We assume the DPC micelle to be a sphere where $R_g^2 = 3R^2/5$ to calculate the micelle radius (R).

Insertion depth: To characterize the relative degree of insertion of $C99_{15-55}$ in the bilayer and micelle, the per residue accessibility of the peptides to water and lipids was computed in terms of the minimum distance of encounter between a given C_α atom to any POPC lipid or DPC surfactant at a given time. The average over time provides a measure of the depth of insertion of the C_α into the water or lipid region.

Coarse-grained model simulations: To construct the CG peptide and bilayer systems, a tool command language (Tcl) script was used to overlap the coordinate files of the peptide and the pre-equilibrated lipid systems and delete the lipid and water residues within 1.5 Å of the CG peptide. The pre-equilibrated boxes were taken from the Marrink website and definitions of all CG particles for the peptide were generated using the Martinize.py script with the MARTINI 2.2 force field for proteins.[12] The CG parameters for lipids, ions, and water molecules were as described by the MARTINI force field.[13] The CG bilayer system consisted of $C99_{15-55}$ monomer, 128 POPC lipids, 1497 water particles, and 3 Cl^- ions to neutralize the system. The CG micelle system contained $C99_{15-55}$ monomer, 54 DPC lipids, 5,597 water particles, and 3 Cl^- ions. For the CG simulations a total of 1 μs of MD were performed on each system. Non-bonded interactions were truncated using shift functions (between 0.9 and 1.2 nm for Lennard-Jones interactions and between 0 and 1.2 nm for electrostatics).[13] The temperature of the systems was set to 303 K using the Berendsen weak coupling method[14] with a coupling time of 0.1 ps. An integration time step of 30 fs was used in all simulations. The pressure was set to 1 bar using a semi-isotropic coupling for POPC and isotropic coupling for DPC using the Berendsen algorithm.

The simulations were carried out using GROMACS (v4.5.1) and the analyses were performed using the GROMACS package, the DSSP program, and tailored scripts using python and MD Analysis libraries.[15–19] Images were generated using VMD.[20] All simulations were performed on the Boston University Katana and SSC supercomputers.

Additional Figures: Fig. 1 shows water and lipid accessibility of each residue of $C99_{15-55}$ in POPC bilayer (above) and DPC micelle (below) generated through all-atom molecular dynamics using the CHARMM36 force field without the CMAP correction. Reasonable agreement is found with the results of all-atom simulations employing the CHARMM36 force field (see Fig 2).

Fig. 2 shows the measurements of the structural kink of each residue of $C99_{15-55}$ in POPC bilayer (above) and DPC micelle (below) generated through all-atom molecular dynamics using the CHARMM36 force field without the CMAP correction. Reasonable agreement is found with the results of all-atom simulations employing the CHARMM36 force field (see Fig.4 and 2.) The kink in the DPC micelle simulations is reduced relative to the corresponding simulations using the CMAP correction.

Fig. 3 shows the distribution of distances between the backbone N atoms of residues G29 and L52 derived from all-atom simulations using the peptide CHARMM36 force field without the CMAP correction. Substantial agreement is found with the results derived from EPR studies (dotted line) of spin-labeled C99 in 1:4 POPG:POPC lipid vesicles. Fig. 4 shows water and lipid accessibility of each residue of $C99_{15-55}$ in POPC bilayer (above) and DPC micelle (below) generated using coarse-grained molecular dynamics using the MARTINI force field and GROMACS. Good qualitative agreement is found between simulations using all-atom (see Fig. 1) and CG (see Fig. 4) models,

[†]Department of Chemistry, Boston University, Boston, MA 02215

[‡]Department of Biochemistry and Molecular Biology and Department of Pathology, The University of Chicago, Chicago, IL 60637

[¶]Department of Chemistry and Biochemistry and Biophysics Program, University of Maryland, College Park, MD 20742

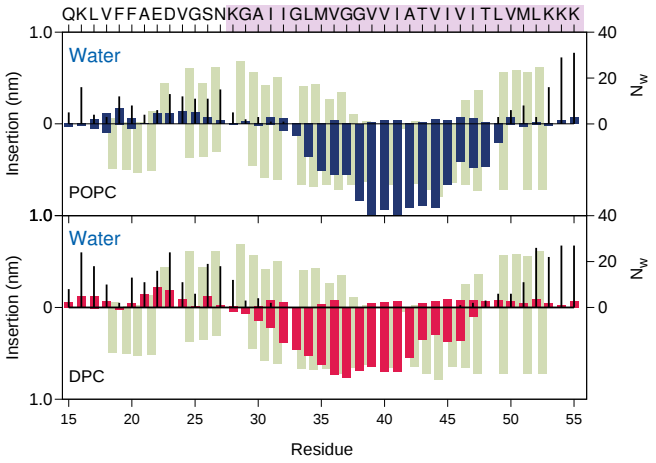

Figure 1. Water and lipid accessibility of each residue of $C99_{15-55}$ in POPC bilayer (above) and DPC micelle (below) derived from all-atom simulations. The grey bars depict the degree of contact with the water-soluble paramagnetic probe (Gd-DTPA, positive values) and the lipophilic probe (16-DSA, negative values) reported by Sanders and coworkers for C99 in LMPG micelles.[1] Shown for comparison are all-atom simulation results using the peptide CHARMM36 force field without the CMAP correction for the depth of insertion in the lipid phase (colored bar) and number of water molecules (black bar) within 4 Å of each amino acid.

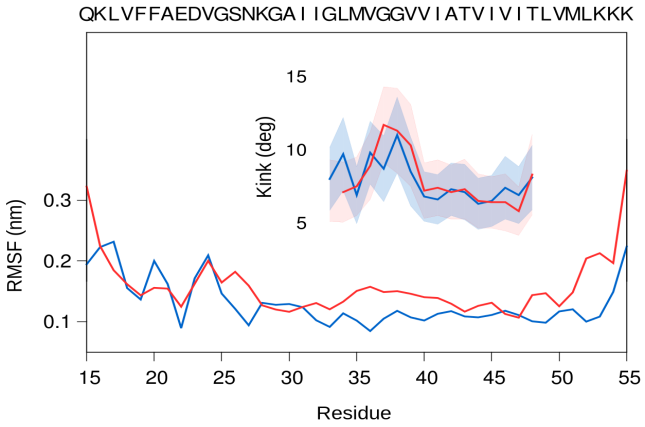

Figure 2. Measurement of the (inset) structural kink derived from all atom simulations using the CHARMM36 force field without the CMAP correction in the peptide and (lower) root-mean-square fluctuations in C_α atoms as a function of residue for the $C99_{15-55}$ monomer in POPC (blue) and DPC (red). Shaded regions indicate ± one standard deviation in uncertainty.

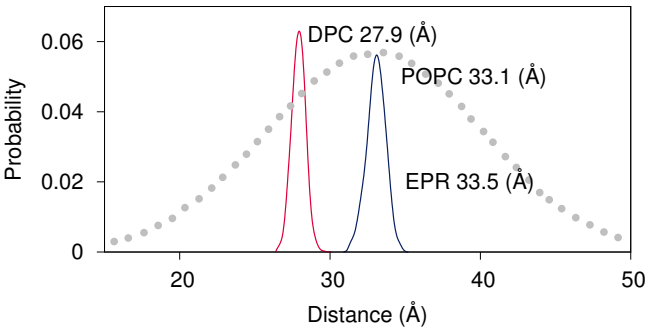

Figure 3. Distribution of distances between the backbone N atoms of residues G29 and L52 derived from all-atom simulations of $C99_{15-55}$ in a DPC micelle and POPC bilayer, compared with experimental results derived from EPR studies (dotted line) of spin-labeled C99 in 1:4 POPG:POPC lipid vesicles.[21]

suggesting self-consistency between the results of the all-atom and CG models. Moreover, there is reasonable agreement between simulation results for $C99_{15-55}$ (in a DPC micelle) and experimental results for full-length C99 (in an LMPG micelle).

Fig. 5 depicts the intramolecular degree of contact between residues of $C99_{15-55}$ in the POPC and DPC simulations and highlights differences in the average structure of the two peptides. In the POPC bilayer relative to the DPC micelle (1) the TM helical region is more extended and stabilized near the C-terminal region and (2) the N-terminal JM helical region is more consolidated. We also note that (3) there is significantly greater interaction between the JM and TM helices in the DPC micelle.

Fig. 6 shows the intramolecular contact map of $C99_{15-55}$ in POPC bilayer (left) and a DPC micelle (right) generated using coarse-grained molecular dynamics using the MARTINI force field and GROMACS. Results for all-atom and CG models lead to similar conclusions. This material is available free of charge via the Internet at `http://pubs.acs.org/`.

References

(1) Beel, A. J.; Mobley, C. K.; Kim, H. J.; Tian, F.; Hadziselimovic, A.; Jap, B.; Prestegard, J. H.; Sanders, C. R. *Biochem.* **2008**, *47*, 9428–9446.
(2) Jo, S.; Kim, T.; Im, W. *PLoS ONE* **2007**, *2*, e880.
(3) Jo, S.; Kim, T.; Iyer, V. G.; Im, W. *J. Comp. Chem.* **2008**, *29*, 1859–1865.
(4) others,, et al. *J. Phys. Chem. B* **1998**, *102*, 3586–3616.
(5) Klauda, J. B.; Venable, R. M.; Freites, J. A.; O'Connor, J. W.; Tobias, D. J.; Mondragon-Ramirez, C.; Vorobyov, I.; MacKerell Jr, A. D.; Pastor, R. W. *J. Phys. Chem. B* **2010**, *114*, 7830–7843.
(6) Huang, J.; MacKerell, A. D. *Journal of Computational Chemistry* **2013**, *34*, 2135–2145.
(7) Abel, S.; Dupradeau, F.-Y.; Marchi, M. *J. Chem. Theor. Compt.* **2012**, *8*, 4610–4623.
(8) Hoover, W. G. *Phys, Rev. A* **1985**, *31*, 1695.
(9) Essmann, U.; Perera, L.; Berkowitz, M. L.; Darden, T.; Lee, H.; Pedersen, L. G. *J. Chem. Phys.* **1995**, *103*, 8577–8593.
(10) Hess, B.; Bekker, H.; Berendsen, H. J.; Fraaije, J. G. *J. Comp. Chem.* **1997**, *18*, 1463–1472.
(11) Bansal, M.; Kumart, S.; Velavan, R. *Journal of Biomolecular Structure and Dynamics* **2000**, *17*, 811–819.
(12) Monticelli, L.; Kandasamy, S. K.; Periole, X.; Larson, R. G.; Tieleman, D. P.; Marrink, S.-J. *J. Chem. Theor. Compt.* **2008**, *4*, 819–834.
(13) Marrink, S. J.; Risselada, H. J.; Yefimov, S.; Tieleman, D. P.; de Vries, A. H. *J. Phys. Chem. B* **2007**, *111*, 7812–7824.
(14) Berendsen, H. J.; Postma, J. P. M.; van Gunsteren, W. F.; DiNola, A.; Haak, J. *J. Chem. Phys.* **1984**, *81*, 3684.
(15) Van Der Spoel, D.; Lindahl, E.; Hess, B.; Groenhof, G.; Mark, A. E.; Berendsen, H. J. *J. Comp. Chem.* **2005**, *26*, 1701–1718.
(16) Hess, B.; Kutzner, C.; Van Der Spoel, D.; Lindahl, E. *J. Chem. Theor. Compt.* **2008**, *4*, 435–447.
(17) Kabsch, W.; Sander, C. *Biopolymers* **1983**, *22*, 2577–2637.
(18) Joosten, R. P.; te Beek, T. A.; Krieger, E.; Hekkelman, M. L.; Hooft, R. W.; Schneider, R.; Sander, C.; Vriend, G. *Nucleic Acids Research* **2011**, *39*, D411–D419.
(19) Michaud-Agrawal, N.; Denning, E. J.; Woolf, T. B.; Beckstein, O. *J. Comp. Chem.* **2011**, *32*, 2319–2327.
(20) Humphrey, W.; Dalke, A.; Schulten, K. *J. Mol. Graph.* **1996**, *14*, 33–38.
(21) Barrett, P. J.; Song, Y.; van Horn, W. D.; Hustedt, E. J.; Schafer, J. M.; Hadziselimovic, A.; Beel, A. J.; Sanders, C. R. *Science* **2012**, *336*, 1168–1171.

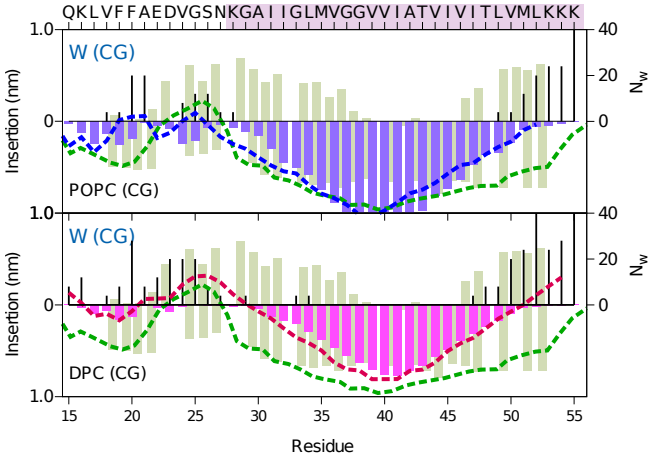

Figure 4. Water and lipid accessibility of each residue of $C99_{15-55}$ in POPC bilayer (above) and a DPC micelle (below) for the CG MARTINI force field. The grey bars depict the degree of contact with the water-soluble paramagnetic probe (Gd-DTPA, positive values) and the lipophilic probe (16-DSA, negative values) reported by Sanders and coworkers [1] for $C99_{15-55}$ in LMPG micelles. Simulation results for the depth of insertion in the lipid phase (colored bar) and number of waters (black bar) are also shown. The water contact was computed by considering all 4 waters composing a water particle to be in contact with a given residue when a water particle was within 5.5 Å of a given protein site. The EPR power saturation data from experimental measurements [21] is presented (green dashed line) and the insertion depth calculated by taking the location of the membrane width or the micelle size for POPC (blue dashed line) and DPC (red dashed line). The TM sequence is marked with orchid shading.

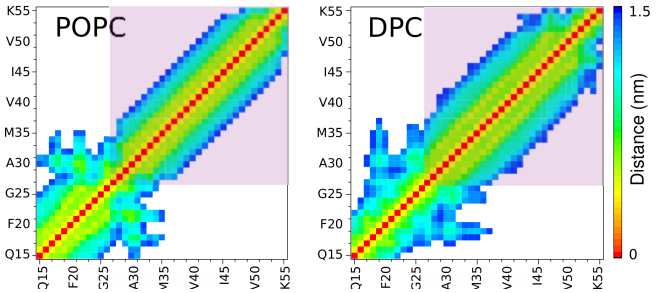

Figure 5. Intramolecular contact map for $C99_{15-55}$ in POPC bilayer (left) and a DPC micelle (right) derived from all-atom simulations using the CHARMM36 peptide force field. The TM region is marked with orchid shading.

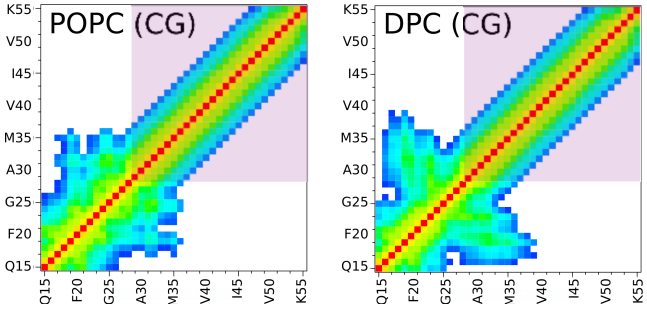

Figure 6. Intramolecular contact map for $C99_{15-55}$ in POPC bilayer (left) and a DPC micelle (right) derived from CG simulations using the MARTINI force field.